

# Structural changes in a metallic glass under cyclic indentation

Karina E. Avila<sup>1</sup> · Vardan Hoviki Vardanyan<sup>1,2,3</sup> · Herbert M. Urbassek<sup>1</sup>

Received: 13 October 2023 / Accepted: 11 November 2023 / Published online: 13 December 2023 © The Author(s) 2023

### **Abstract**

Using molecular dynamics simulation, a CuZr metallic glass was subjected to cyclic indentation to investigate cyclic hardening. Structural changes occurring after each indentation cycle were analyzed by examining the radial changes of the structural motifs in the vicinity of the indenter surface. The analysis revealed initial local structural modifications that corresponded to a more relaxed glass state, followed by a slow restoration of the initially destroyed structures. These findings provide new insights into the microstructural causes of cyclic hardening in metallic glasses.

Keywords Cyclic nanoindentation · Hardness · Shear transformation zones · Molecular dynamics

# 1 Introduction

In metallic glasses (MGs), the phenomenon of cyclic hardening is characterized by an enhancement in the material strength and resistance to deformation when subjected to repeated loading cycles [1–5]. This effect progressively develops over multiple cycles until a saturation point is reached. Both experimental [1, 2] and molecular dynamics simulations [3–5] have demonstrated this phenomenon, which is applicable across a broad spectrum of MG compositions and temperatures.

Simulation outcomes propose that the hardening is triggered by confined microplasticity and stiffening in regions of the originally preferred yielding path, necessitating a higher applied load to initiate a secondary path [2, 4]. However, the structural modifications leading to local hardening remain unclear. Existing tools have been unable to provide clear indications of any changes induced by cycling [2].

The mechanical properties of MGs are largely governed by local atomic structures, referred to as short-range order motifs [6–8]. These motifs, acting as the closest neighboring elements of the glass, exhibit a distinct structural hierarchy dependent on the coordination number of the central atom. The full-icosahedral (FI) clusters centered on Cu atoms have been identified as the most relevant motif. During mechanical deformation, significant deformation of these motifs has been observed [9–11], particularly the FI motifs [10, 12–14].

In this study, we perform simulations of a CuZr MG subjected to cyclic indentation. We examine the radial alterations of the motifs in relation to the indenter surface to identify any discernible structural changes that could elucidate the microstructural causes of cyclic hardening. Our analysis uncovers initial local structural modifications corresponding to a more relaxed glass state. Subsequent cyclic measurements indicate a partial restoration of the initially destroyed structures. However, this recovery process saturates after the fifth cycle.

### 2 Simulation details

In this research, a CuZr glass with a composition of  $Cu_{64.5}$  Zr<sub>35.5</sub> was used. The glass was produced by melting a crystalline mixture at a temperature of  $T_m = 2000$  K for 500 ps, then cooled to room temperature (T = 300 K) at a quenching rate of 0.01 K/ps, and relaxed for 200 ps under periodic boundary conditions. More information on sample preparation can be found in Refs. [15, 16]. The simulation was carried out in a cubic box with a length of L = 45 nm, containing 5 619 712 atoms.



Herbert M. Urbassek urbassek@rhrk.uni-kl.de

Physics Department and Research Center OPTIMAS, RPTU Kaiserslautern, Erwin-Schrödinger-Straße, 67663 Kaiserslautern, Germany

Department of Chemistry, Rice University, Houston, TX 77005, USA

<sup>&</sup>lt;sup>3</sup> Center for Theoretical Biological Physics, Rice University, Houston, TX 77005, USA

Before cyclic indentation, the sample was relaxed for an additional 300 ps under periodic boundary conditions in the lateral directions and free boundary conditions on the top surface. During indentation, the temperature of the sample was kept at 300 K using an NVT ensemble for ten indentation cycles. A 1-nm layer at the bottom of the samples was fixed, simulating an immobile bulk MG. The indenter had a spherical shape with a radius of R = 10 nm and stiffness constant of K = 10 eV/Å[17], interacting repulsively with the sample and moving in the -z direction at a velocity of 20 m/s.

The first indentation cycle penetrated the sample down to 7 nm. The force acting on the indenter at this depth was then used as a control value for the next nine cycles, such that the indentation depth of the ensuing cycles could not change, while the maximum normal force was fixed. After retraction of the indenter, the next cycle was started as soon as the indenter lost contact with the sample and the normal force on the indenter vanished.

The open-source visualization tool OVITO [18] was utilized to analyze the plasticity created on the samples by the indentation procedure.

### 3 Results

### 3.1 Virgin sample

Prior to indentation, a sample analysis is conducted to determine the total number of the most common motifs which are organized according to their coordination number (CN) in Fig. 1. The color distinction in the figure signifies whether the cluster is centered around a Copper (Cu) atom—depicted in blue—or around a Zirconium (Zr) atom—depicted in

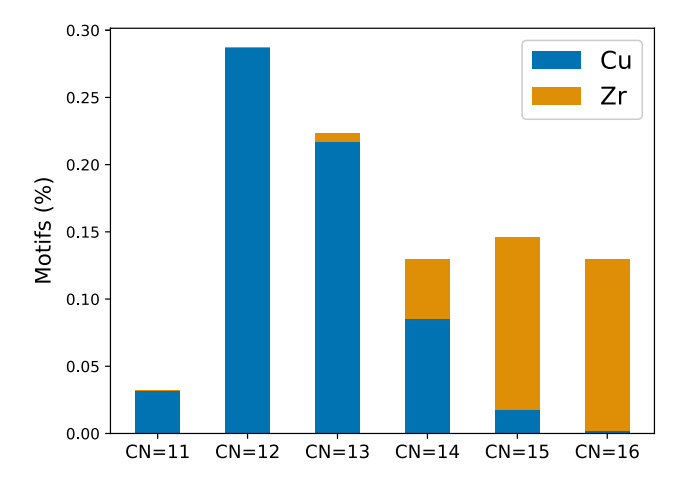


**Fig. 1** Distribution of motifs, classified by their coordination number CN, in the virgin sample before indentation takes place. The color differentiates whether the cluster is centered around a Cu (blue) or Zr (orange) atom

orange. The figure reveals that motifs with CN = 12 are the most common. This category includes full icosahedral (FI) motifs (0,0,12,0), which have been associated with structural stability [8]. This figure also shows that motifs with large CN>15 are predominantly Zr-centered, while those with smaller CNs are primarily Cu-centered. This finding is in agreement with the larger atomic size of the Zr atom as compared to the Cu atom and is in agreement with the previous studies [19, 20].

# 3.2 Structural modification after the first indentation cycle

Upon completion of the initial indentation cycle, we proceeded to examine the resulting plasticity. In Fig. 2, the von-Mises shear strain (VMSS) is displayed for a cross section of the sample. This figure reveals that the most significant plasticity is primarily concentrated near the indenter. The observed plasticity is largely composed of shear transformation zones, which are localized plastic shear events involving approximately 100 atoms [21]. No shear bands were localized.

To analyze the plasticity in a more qualitative manner, the plastic zone beneath the indenter was divided into radial layers of 5 Å each. The radial coordinate  $r_a$  measures the distance of these layers to the indenter surface. To measure averaged quantities within these layers, a method similar to the one described in Ref. [22] is employed. These measurements were performed at the maximum depth of indentation, just prior to the removal of the indenter. Furthermore, all results presented henceforth are determined relative to

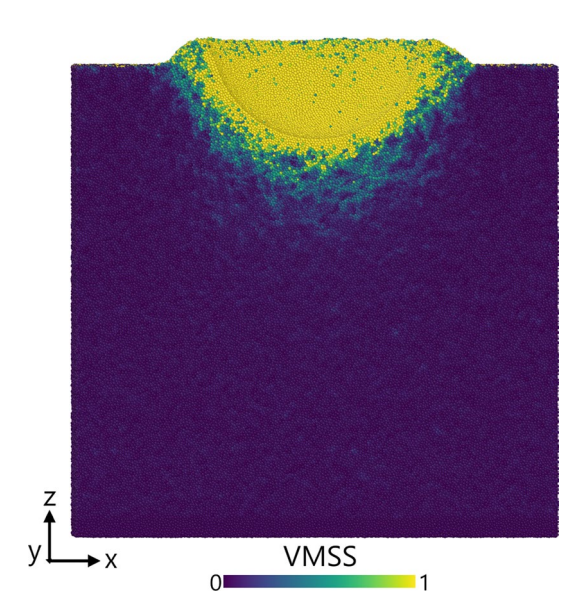


**Fig. 2** Cross-sectional snapshot of the sample after the first indentation with an indenter of radius R = 10 nm to a depth of 7 nm. Atoms are color-coded according to their VMSS values



the initial atomic configuration, before the initiation of the indentation process. For this analysis, the first radial layer directly below the indenter was ignored, as this is the point where the most changes occur and it obscures the other results. The focus is mostly on the radial progress. The surface and pile-up were also ignored, meaning that only atoms below a depth of 6 Å beneath the surface were considered.

Figure 3 displays the radial change of the VMSS and the percent change with respect to the virgin sample of FI motifs. The maximum change in FI reached is close to the indenter, with almost an 8% destruction of FI. This figure indicates that the FI % change and the VMSS almost reach

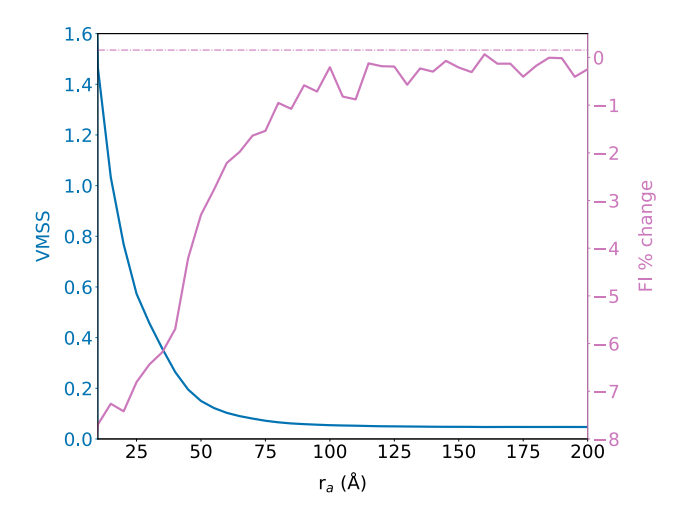


Fig. 3 Radial dependence of the VMSS (left axis) and of the percent change of the full-icosahedral (FI) motifs after the first indentation. The radial coordinate  $r_a$  measures the distance of these layers to the indenter surface. The data were taken at the maximum depth of indentation

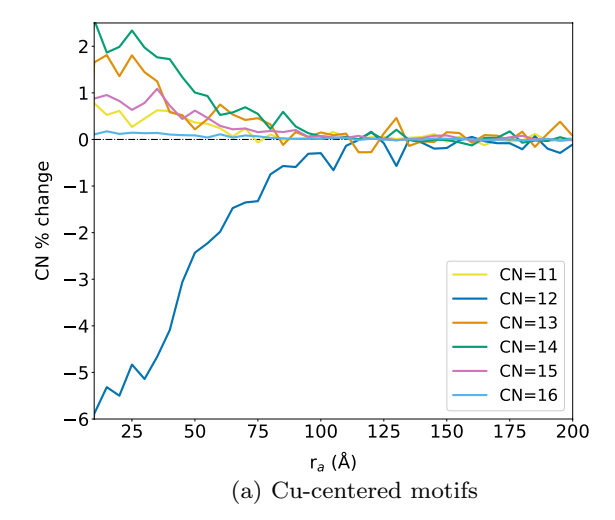
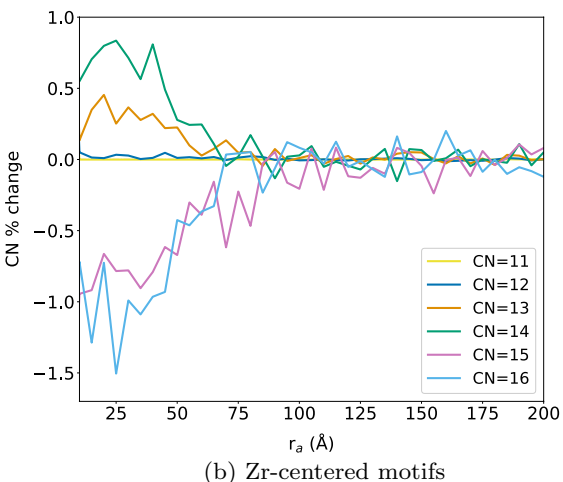


Fig. 4 Percentage change of the motifs with coordination number CN as a function of the radial distance  $r_a$  to the indenter surface. These data were taken at the point of maximum indentation depth. Data are

0 values around 100 Å, which suggests the extent of the plastic zone.

In addition to the FI motifs, the radial dependence of the remaining motifs, differentiated by their CN, was investigated. Figure 4 shows this dependence, further categorized by whether the motifs are centered around Cu, Fig. 4a, or Zr, Fig. 4b. The data reveal that Cu-centered motifs with a CN of 12 exhibit the most significant changes; more than 5% are destroyed in regions near the indenter surface. A comparison with Fig. 3 suggests that these changes predominantly occur within the FI. Other Cu-centered motifs demonstrate an increase across the remaining motifs. For Zr-centered motifs, those with higher coordination numbers (CNs >15) display a destruction fraction of nearly 1%. The remaining Zr-centered motifs exhibit an increase in their population. A closer inspection of the changes in the cluster populations based on their coordination numbers and elemental centers reveals the following features.

- For CN=11, Cu-centered motifs exhibit an increase of less than 1%, while Zr-centered motifs remain unchanged.
- 2. As previously noted, Cu-centered motifs with CN=12 show a decrease exceeding 5%, whereas Zr-centered motifs display negligible change.
- 3. For CN = 13 and CN = 14, both Cu- and Zr-centered motifs show an increase in population. The increase is more pronounced for Cu-centered motifs, with a rise of nearly 2% for both CN = 13 and CN = 14. In contrast, Zr-centered motifs show a more modest increase of approximately 0.75% for CN = 13 and 0.3% for CN = 14.



given for (a) Cu-centered and (b) Zr-centered motifs after the first indentation with respect to the virgin sample



4. For motifs with CN = 15 and 16, there is a decrease of approximately 1% for Zr-centered motifs. In contrast, Cu-centered motifs display an increase of 1% for CN = 15, while CN = 16 shows virtually no change.

Moreover, Cu-centered motifs with CN = 12 appear to have a more extensive range effect. They approach zero in the range between 100–125 Å below the indenter's surface. In contrast, the rest of the motifs, including all Zr-centered motifs, seem to reach the zero line earlier, around 75 Å below the surface.

Overall, following the initial cycle, we observed alterations in the CN that are consistent with a more rejuvenated sample, as seen at lower temperatures [10]. This rejuvenation is characterized by a marked decrease in CN=12 and an increase in CN=14 for this specific stoichiometry. These changes are concentrated in the vicinity of the indenter, leading to substantial modifications in its structural characteristics. Rejuvenation effects similar to those observed in our study were also noted in experiments involving cryogenic cycle treatments [23].

## 3.3 Cyclic hardening

The focus now shifts to the outcomes of conducting nine additional indentations following the initial indentation cycle. Figure 5 presents the indentation force across the ten indentation cycles. It is clear from this figure that applying consistent force in subsequent indentations results in negligible variation in the indentation depth, as evidenced by the indistinguishable nature of the subsequent indentations. The precise value of the maximum indentation depth achieved in each indentation cycle is shown in Fig. 6. This figure reveals

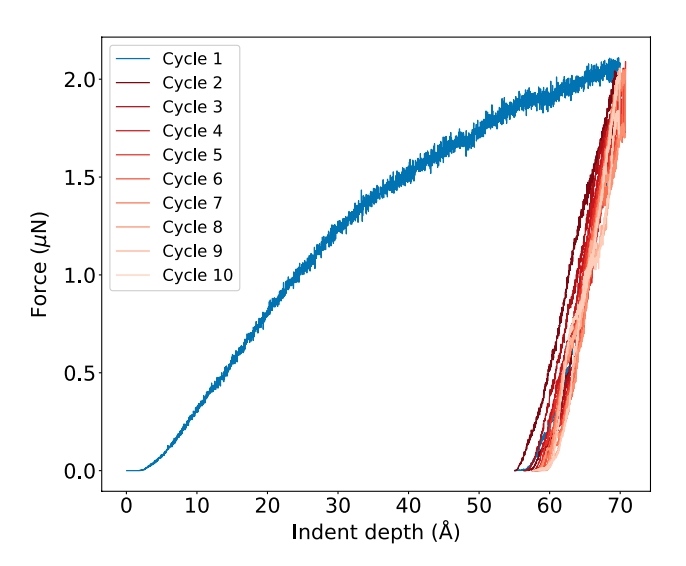


Fig. 5 Dependence of the normal force on the indentation depth for all the ten indentation cycles



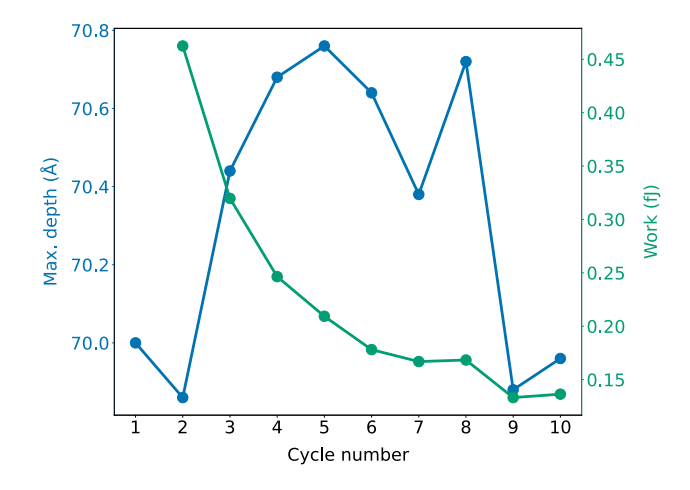


Fig. 6 Dependence of the maximum indentation depth (left axis) and of the plastic work done (right axis) as a function of the indentation cycle

that not only was the change in maximum indentation depth confined within a 1 Å range, but it also exhibited a decrease post the fifth indentation, nearing 70 Å once again.

Furthermore, Fig. 6 illustrates the work required to perform these indentations, which is defined as the area encompassed between the loading and unloading curves. The size of the hysteresis loop serves as a measure of the amount of plastic work carried out in each cycle [24]. A contraction in the hysteresis loop size implies a reduction in energy dissipation via irreversible deformation, suggesting a decrease in plastic deformation of the material [25]. This could be attributed to a multitude of factors, including modifications in the microstructural characteristics of the material. Interestingly, a consistent decrease in work with each subsequent indentation cycle is observed. This trend is also indicative of hardening with each additional indentation. This means that the material becomes more resistant to deformation with each cycle. As a result, a diminished amount of work—or energy—is demanded to achieve the same indentation depth in subsequent cycles. This is demonstrated by the shrinking area between the loading and unloading curves, which signifies the work conducted during indentation.

It is essential to emphasize that the behavior observed in this study can be influenced by a multitude of factors. These include the specific composition of the MG, the loading rate, and other conditions associated with experimental or simulation settings. Despite the potential variability introduced by these factors, a degree of consistency has been detected across different conditions. For instance, similar results were observed at a lower temperature ( $T = 0.1 \,\mathrm{K}$ ) for this stoichiometry [5], thereby strengthening these findings. The findings presented in this study are also consistent with earlier results found in both simulations [3–5] and experiments [1, 2]. However, despite these results being observed

across a wide spectrum of conditions, the microstructural elements that trigger this phenomenon are yet to be determined. Therefore, in the following section, we conduct an analysis of the structural changes in the glass, after subsequent indentation cycles, with the aim of identifying the underlying cause of cyclic hardening.

## 3.4 Structural modification up to the tenth cycle

We now shift our focus to the analysis of structural modifications following the subsequent indentations. To maintain simplicity in this analysis, we will only take into account the alterations observed in cycles 5 and 10 in comparison to cycle 1, which has been previously addressed in Sect. 3.2. The radial dependency of the VMSS is shown in Fig. 7. This figure reveals an increase in the average VMSS from cycle 1 to cycle 5. However, it shows that the VMSS exhibits negligible variations between cycles 5 and 10, indicating a stable state of plasticity. Also, at distances > 60 Å below the indenter surface, the averaged VMSS is around 0.1, which signifies very low plasticity.

Analogous to the analysis of structural changes conducted for cycle 1 in Sect. 3.2, we also track the radial changes of these motifs for cycles 5 and 10 to observe their evolution.

The individual examination of changes between cycles for different CNs of Cu-centered motifs is depicted in Fig. 8. As before, the changes are given with respect to the virgin sample. The following observations can be made from this figure.

(a) CN = 11: There is no discernible pattern between the different cycles. It appears that there is no significant

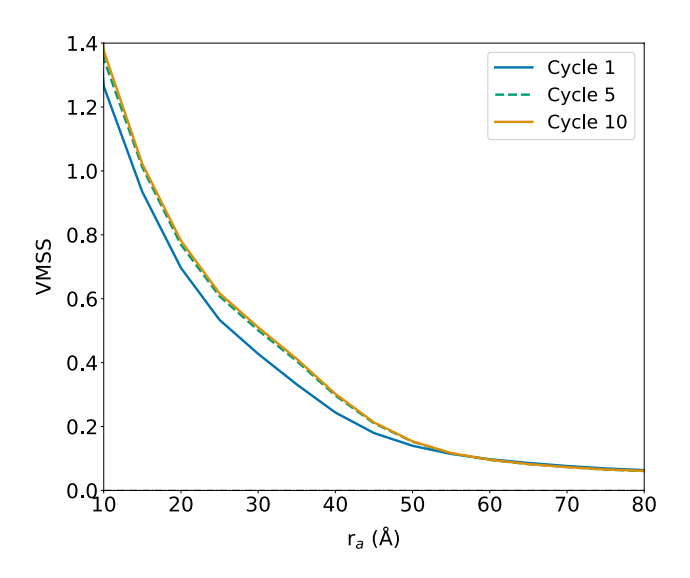


**Fig. 7** Radial dependence of the VMSS for indentation cycles 1, 5 and 10, with data taken at the deepest point of indentation

- change, and most of the alterations occur between the lavers, i.e., fluctuations.
- (b) CN = 12: There is a recovery of approximately 2% between cycle 1 and cycle 5 of the previously broken motifs. No significant changes are observed between cycle 5 and cycle 10.
- (c) CN = 13: Similar to CN = 11, there is no evident change between the different cycles.
- (d) CN = 14: There is a destruction of less than 1% in the cluster formed in cycle 1 from cycle 1 to cycle 5. An additional change of about 0.5% occurs between cycle 5 and cycle 10.
- (e) CN = 15: Similar to CN = 14, there is a decrease in the population of motifs formed during cycle 1. The decrease is not significant, around 0.5%, and there are no apparent changes between cycle 5 and cycle 10 outside fluctuations.
- (f) CN = 16: There is a decrease in the population of motifs of approximately 0.05% after cycle 5 and an additional decrease of also approximately 0.05% after cycle 10. The aforementioned changes occur only in intermediate layers 25 Å <  $r_a$  < 75 Å.

In a similar manner, we can investigate the variations between cycles of different CNs, but this time for Zr-centered motifs, as illustrated in Fig. 9. The following deductions can be made from this figure.

- (a) CN = 11: No discernible change.
- (b) CN = 12: No clear variation is observed between the different cycles apart from fluctuations.
- (c) CN = 13: A systematic yet minimal decrease in the motifs, around 0.1%, appears to transpire after subsequent indentations.
- (d) CN = 14: No significant change is observed beyond fluctuations.
- (e) CN = 15: An increase in the cluster population of more than 0.5% seems to occur; however, this is only evident for the first layers  $r_a < 25 \text{ Å}$ .
- (f) CN = 16: A minor increase in the motifs appears to occur after cycle 5; however, the change is more pronounced in the middle layers  $r_a > 35$  Å. In the first layers, the population decreased after cycle 5 but then increases after cycle 10. In the middle layers, no significant changes are observed between cycle 5 and cycle 10.

# 4 Summary and conclusions

In this study, to further elucidate the phenomenon of cyclic hardening in metallic glasses, we executed cyclic indentation on a CuZr MG under room-temperature conditions. We



**22** Page 6 of 8 K. E. Avila et al.

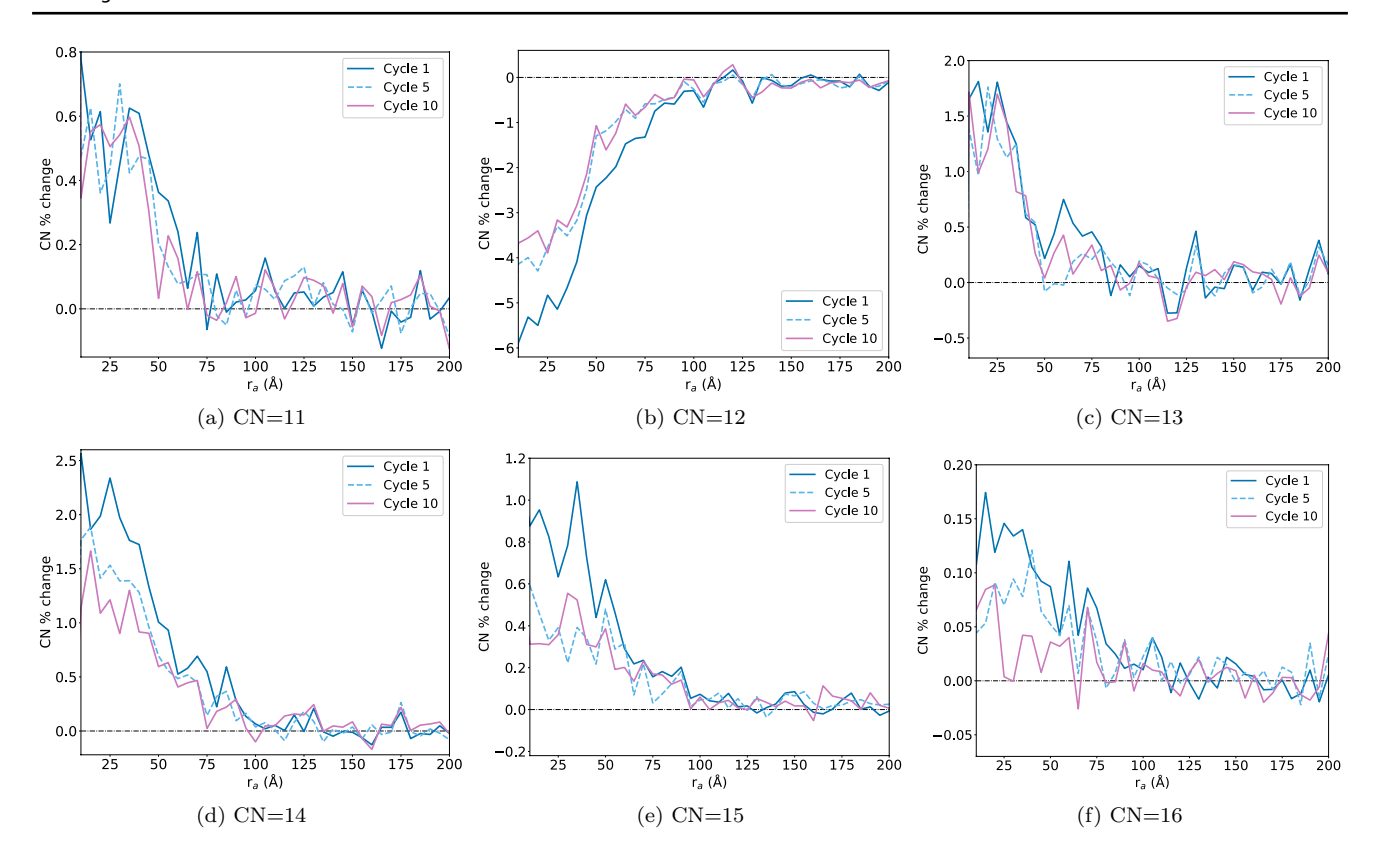


Fig. 8 Percentage change of the Cu-centered motifs with coordination number CN as a function of the radial distance  $r_a$  to the indenter surface. These data were taken at the maximum indentation depth for

each cycle. Data are given for after the first, fifth and tenth indentation with respect to the virgin sample

analyzed the structural alterations occurring in the plastic zone proximal to the indenter. Specifically, we investigated the alterations that occurred in Cu-centered motifs and Zr-centered motifs individually, across radial layers around the indenter.

Overall, our study revealed that during cyclic indentation, specific motifs, particularly those centered around Cu with a CN of 12 and Zr with CNs of 15 and 16, were destroyed in the first indentation cycle. However, these motifs exhibited a recovery in subsequent cycles. Conversely, other motifs, specifically those centered around Cu excluding CNs of 11 and 13, and Zr with CNs of 12, 13, and 14, demonstrated an increase following the first indentation. These motifs then exhibited a decrease in subsequent cycles.

The structural transformations ensuing the initial indentation cycle thus culminated in a glass state that was more rejuvenated compared to its pre-indentation state. This dynamic phenomenon of motif destruction and restoration suggests an atomic-level 'push-pull' effect. The destruction of a motif (or 'push') necessitates energy for its restoration (or 'pull') to its original state. In contrast, an increase in a motif (or 'pull') requires energy for its decrease (or 'push'). This continuous 'push-pull' process during cyclic

indentation could be the reason for the substantial energy requirement for further transformations.

This interplay could have profound implications for the properties and applications of MGs. For example, insights into how MGs react to repeated mechanical stress at the atomic level could guide strategies to improve their durability or resilience. Additional research would be required to fully comprehend these processes and their implications.

Some evidence was found that the most stable motifs, the Cu-centered motifs with CN = 12 which include the full icosahedrals, are destroyed in a slightly wider environment of the indenter than the other motifs. Even though this result appears to be at the limit of our statistical reliability, it thus appears that the destruction of motifs with CN = 12 precedes the modification of the other motifs.

Overall, the structural changes in the sample reached saturation after the fifth cycle. This is in agreement with the stabilization of the plastic work done in the later indentation cycles determined via the indentation—retraction hysteresis, as was shown in Fig. 6. Note that the occurrence of thermal processes, which might lead to structural changes between the individual cycles, is highly improbable as our indentations follow each other without delay.



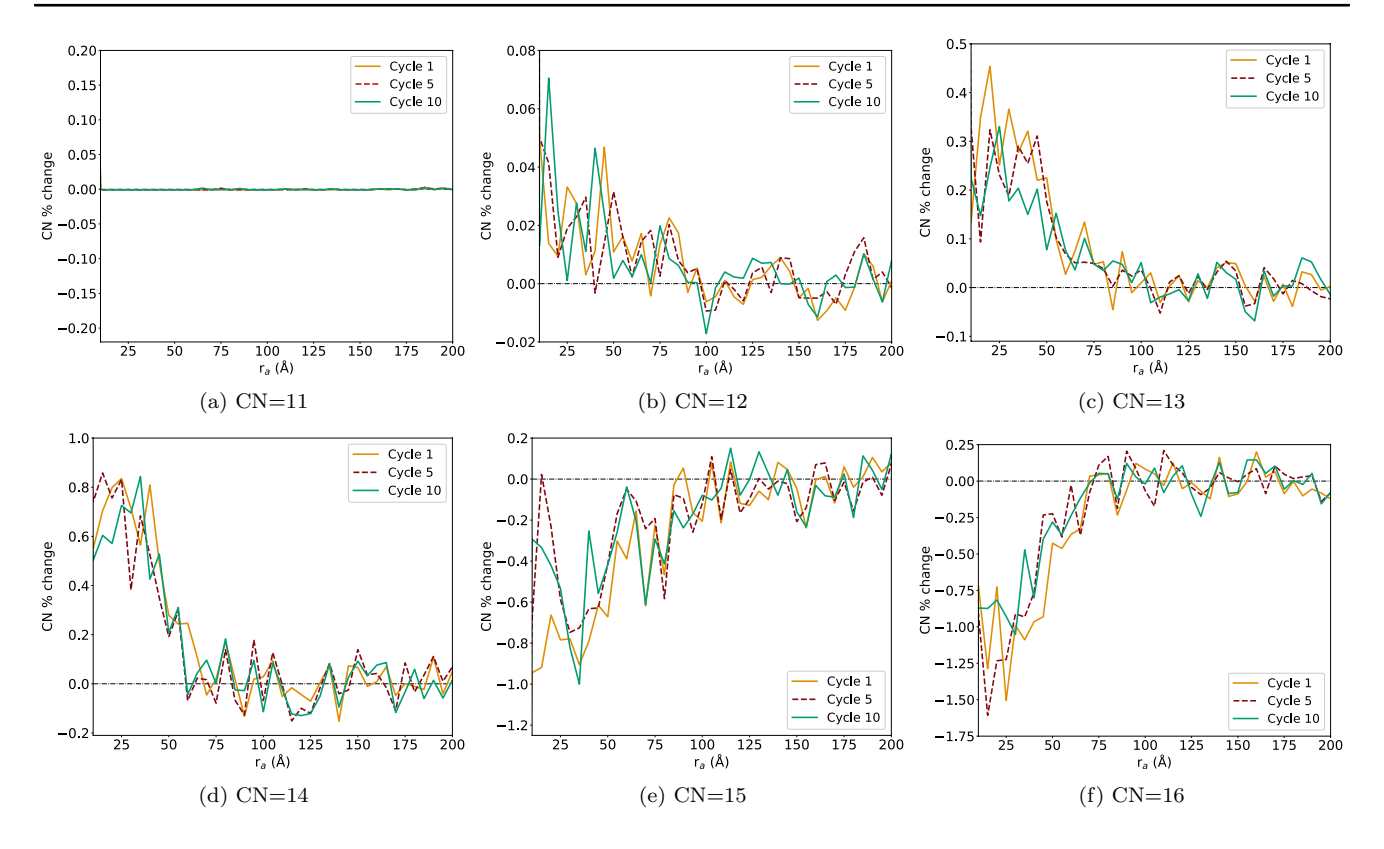


Fig. 9 As in Fig. 8, but for Zr-centered motifs. Data were taken at the maximum indentation depth for each cycle

Finally, the macroscopic measurements presented in this manuscript correspond well with the experimental findings reported in Ref. [5]. This congruence is apparent in the trends seen in changes in indentation depth and hysteresis over multiple indentation cycles. It is essential to emphasize this aspect, as experimental techniques do not allow for the detection of microscopic changes in the structure that can be observed through simulations. Therefore, simulations like the one conducted in this study are indispensable in supplementing experimental research, especially in the domain of the plastic analysis of metallic glasses.

**Acknowledgements** Access to the computational resources provided by the compute cluster "Elwetritsch" of the RPTU is appreciated.

**Author contributions** All authors designed the study. VV and KA performed the simulations and analyzed the results. KA wrote the manuscript. All authors discussed the results and reviewed the manuscript.

Funding Open Access funding enabled and organized by Projekt DEAL.

Data availability All data used for this study are contained in this article

### **Declarations**

**Conflict of interest** The authors declare that they have no known competing financial interests or personal relationships that could have appeared to influence the work reported in this paper.

Open Access This article is licensed under a Creative Commons Attribution 4.0 International License, which permits use, sharing, adaptation, distribution and reproduction in any medium or format, as long as you give appropriate credit to the original author(s) and the source, provide a link to the Creative Commons licence, and indicate if changes were made. The images or other third party material in this article are included in the article's Creative Commons licence, unless indicated otherwise in a credit line to the material. If material is not included in the article's Creative Commons licence and your intended use is not permitted by statutory regulation or exceeds the permitted use, you will need to obtain permission directly from the copyright holder. To view a copy of this licence, visit <a href="http://creativecommons.org/licenses/by/4.0/">http://creativecommons.org/licenses/by/4.0/</a>.

### References

- C.E. Packard, E.R. Homer, N. Al-Aqeeli, C.A. Schuh, Cyclic hardening of metallic glasses under Hertzian contacts: Experiments and STZ dynamics simulations. Philos. Mag. 90, 1373–1390 (2010). https://doi.org/10.1080/14786430903352664
- C.E. Packard, L.M. Witmer, C.A. Schuh, Hardening of a metallic glass during cyclic loading in the elastic range. Appl. Phys. Lett. 92, 171911 (2008). https://doi.org/10.1063/1.2919722



**22** Page 8 of 8 K. E. Avila et al.

 C. Deng, C.A. Schuh, Atomistic mechanisms of cyclic hardening in metallic glass. Appl. Phys. Lett. 100, 251909 (2012). https:// doi.org/10.1063/1.4729941

- D. Zhao, H. Zhao, B. Zhu, S. Wang, Investigation on hardening behavior of metallic glass under cyclic indentation loading via molecular dynamics simulation. Appl. Surf. Sci. 416, 14–23 (2017). https://doi.org/10.1016/j.apsusc.2017.04.125
- K.E. Avila, V.H. Vardanyan, T. Zhu, S. Küchemann, M. Smaga, H.M. Urbassek, "Plasticity in cyclic indentation of a Cu-Zr-based bulk metallic glass after tensile loading: An experimental and molecular dynamics simulation study," Journal of Non-Crystalline Solids 617, 122486 (2023). https://doi.org/10.1016/j.jnoncrysol. 2023.122486
- Y.Q. Cheng, E. Ma, Indicators of internal structural states for metallic glasses: Local order, free volume, and configurational potential energy. Appl. Phys. Lett. 93, 051910 (2008). https://doi. org/10.1063/1.2966154
- Z.D. Sha, Y.P. Feng, Y. Li, Statistical composition-structureproperty correlation and glass-forming ability based on the full icosahedra in Cu-Zr metallic glasses. Appl. Phys. Lett. 96, 061903 (2010). https://doi.org/10.1063/1.3310278
- E. Ma, Tuning order in disorder. Nat. Mater. 14, 547–552 (2015). https://doi.org/10.1038/nmat4300
- T. Egami, W. Dmowski, C.W. Ryu, Medium-range order resists deformation in metallic liquids and glasses. Metals 13, 442 (2023). https://doi.org/10.3390/met13030442
- K.E. Avila, S. Küchemann, R.E. Pinzón, H.M. Urbassek, Influence of stoichiometry on indentation-induced plasticity in CuZr glasses. Appl. Phys. A 127, 702 (2021). https://doi.org/10.1007/s00339-021-04856-4
- G. Wang, N. Mattern, J. Bednarčí, L. Xia, Q.J. Zhai, Y.D. Dong, J. Eckert, Deformation induced structural evolution in bulk metallic glasses. Chin. Sci. Bull. 56, 3952–3959 (2011). https://doi.org/10.1007/s11434-011-4784-5
- J. Zemp, M. Celino, B. Schönfeld, J.F. Löffler, Crystal-like rearrangements of icosahedra in simulated copper-zirconium metallic glasses and their effect on mechanical properties. Phys. Rev. Lett. 115, 165501 (2015). https://doi.org/10.1103/PhysRevLett. 115.165501
- K.E. Avila, S. Küchemann, H.M. Urbassek, Interaction between parallel shear bands in a metallic glass. J. Non-Cryst. Solids 566, 120882 (2021). https://doi.org/10.1016/j.jnoncrysol.2021.120882
- K.E. Avila, S. Küchemann, I. Alabd Alhafez, H.M. Urbassek, An atomistic study of shear-band formation during cutting of metallic glasses. J. Appl. Phys. 127, 115101 (2020). https://doi.org/10. 1063/1.5141336
- K.E. Avila, S. Küchemann, I. Alabd Alhafez, H.M. Urbassek, Shear-transformation-zone activation during loading and

- unloading in nanoindentation of metallic glasses. Materials **12**, 1477 (2019). https://doi.org/10.3390/ma12091477
- K.E. Avila, S. Küchemann, I. Alabd Alhafez, H.M. Urbassek, Nanoscratching of metallic glasses – an atomistic study. Tribol. Int. 139, 1–11 (2019). https://doi.org/10.1016/j.triboint.2019.06. 017
- C.L. Kelchner, S.J. Plimpton, J.C. Hamilton, Dislocation nucleation and defect structure during surface indentation. Phys. Rev. B 58, 11085–11088 (1998). https://doi.org/10.1103/PhysRevB.58. 11085
- A. Stukowski, Visualization and analysis of atomistic simulation data with OVITO – the Open Visualization Tool. Model. Simul. Mater. Sci. Eng. 18, 015012 (2010). https://doi.org/10.1088/0965-0393/18/1/015012. http://www.ovito.org/
- M. Li, C. Z. Wang, S. G. Hao, M. J. Kramer, K. M. Ho, "Structural heterogeneity and medium-range order in Zr<sub>x</sub>Cu<sub>100-x</sub> metallic glasses," Phys. Rev. B 80, 184201 (2009). https://doi.org/10.1103/PhysRevB.80.184201
- J. Ding, Y.-Q. Cheng, E. Ma, Full icosahedra dominate local order in Cu<sub>64</sub>Zr<sub>34</sub> metallic glass and supercooled liquid. Acta Mater. 69, 343–354 (2014). https://doi.org/10.1016/j.actamat.2014.02.005
- A.L. Greer, Y.Q. Cheng, E. Ma, Shear bands in metallic glasses. Mater. Sci. Eng. R. Rep. 74, 71–132 (2013). https://doi.org/10. 1016/j.mser.2013.04.001
- K.E. Avila, S. Küchemann, H.M. Urbassek, Structure and size of the plastic zone formed during nanoindentation of a metallic glass. J. Non-Cryst. Solids 523, 119593 (2019). https://doi.org/10. 1016/j.jnoncrysol.2019.119593
- Z. Peng, Y. Chen, G. Yin, P. Gong, Z. Jamili-Shirvan, N. Li, X. Wang, K. Yao, Effect of cryogenic cycling on mechanical properties of ZrTiCuNiBe bulk metallic glass. Fundamental Research 2, 764–775 (2022). https://doi.org/10.1016/j.fmre.2021.11.026
- 24. J. Polák, R. Petráš, "Hysteresis loop analysis in cyclically strained materials," in *Inelastic Behavior of Materials and Structures Under Monotonic and Cyclic Loading*, edited by Holm Altenbach and Michael Brünig (Springer International Publishing, Cham, 2015) pp. 185–205. https://doi.org/10.1007/978-3-319-14660-7\_10
- S. Deldar, I. Alabd Alhafez, M. Smaga, T. Beck, H.M. Urbassek, Cyclic indentation of iron: A comparison of experimental and atomistic simulations. Metals 9, 541 (2019). https://doi.org/10. 3390/met9050541

**Publisher's Note** Springer Nature remains neutral with regard to jurisdictional claims in published maps and institutional affiliations.

